Solar Phys (2018) 293:95
https://doi.org/10.1007/s11207-018-1313-6

Fragile Detection of Solar *g*-Modes by Fossat *et al.*

Hannah Schunker[1] · Jesper Schou[1] · Patrick Gaulme[1] · Laurent Gizon[1,2]

Received: 12 April 2018 / Accepted: 31 May 2018 / Published online: 21 June 2018

Abstract The internal gravity modes of the Sun are notoriously difficult to detect, and the claimed detection of gravity modes presented by Fossat *et al.* (*Astron. Astrophys.* **604**, A40, 2017) is thus very exciting. Given the importance of these modes for understanding solar structure and dynamics, the results must be robust. While Fossat *et al.* described their method and parameter choices in detail, the sensitivity of their results to several parameters was not presented. Therefore, we test the sensitivity of the results to a selection of the parameters. The most concerning result is that the detection vanishes when we adjust the start time of the 16.5-year velocity time-series by a few hours. We conclude that this reported detection of gravity modes is extremely fragile and should be treated with utmost caution.

Keywords Helioseismology, observations · Interior · Oscillations

1. Introduction

Despite the revelations about the solar internal structure and dynamics from helioseismology in the past 30 years, the deep core of the Sun has remained invisible. This is because the most easily observed pressure modes (p-modes) are predominantly sensitive to the near-surface layers of the Sun. Gravity modes (g-modes) that probe the core of the Sun are evanescent in the convection zone and have small predicted amplitudes at the surface, making them difficult to detect (*e.g.* Appourchaux *et al.*, 2010). There have been prior claims of g-mode detection, *e.g.* García *et al.* (2007), but to our knowledge, the results have not been reproduced using independent observations, and they remain controversial. Refreshingly, Fossat *et al.* (2017) provided their data publicly and described their method sufficiently well for us to qualitatively reproduce their results.

✉ H. Schunker
schunker@mps.mpg.de

1 Max-Planck-Institut für Sonnensystemforschung, Justus-von-Liebig-Weg 3, 37077 Göttingen, Germany

2 Institut für Astrophysik, Georg-August-Universität Göttingen, Friedrich-Hund-Platz 1, 37077 Göttingen, Germany

Fossat *et al.* (2017) presented a method based on the principle that g-modes perturb the solar core, changing the round-trip travel-time (the time taken to travel to the other side of the Sun and back) of the sound waves (p-modes). They measured perturbations to the large separation (equivalent to the round-trip travel-time) between pairs of low-frequency p-modes with even ($\ell = 0, 2$) and odd ($\ell = 1-3$) harmonic degrees. The large separation is not as susceptible to convective noise and surface effects as individual mode frequencies, and it is sensitive to the mean density of the Sun.

Applying their method to the long-term velocity time-series from the *Global Oscillations at Low Frequencies* (GOLF: Gabriel *et al.*, 1995) instrument, Fossat *et al.* (2017) inferred that the solar core rotates about 3.8 times faster than the envelope. Given the potential impact of this detection on our understanding of solar structure and dynamics, it is important that these results can be independently reproduced and tested. A robust detection would also affect the theory of stellar evolution, and the method could potentially be applied to stellar observations of Sun-like stars, for example from *PLAnetary Transits and Oscillations of stars* (PLATO: Rauer *et al.*, 2014) observations.

Although Fossat *et al.* (2017) described their analysis method well enough for it to be qualitatively reproduced, they did not present a quantitative description of the sensitivity to the parameters of the method.

In this article we first present our independent reproduction of the measurement of the rotational splitting of the g-modes (Section 2). We then examine the sensitivity of the significance of the detection to four parameters in the analysis method: the method used to measure the round-trip travel-time in Section 3, the smoothing of the power spectrum of the round-trip travel-time in Section 4, the cadence of the start-time of the GOLF time series in Section 5, and the round-trip travel-time measurements in Section 6. We conclude in Section 7.

2. Reproduction of g-Mode Detection

By following the analysis method described by Fossat *et al.* (2017), we were able to qualitatively reproduce the results of Figure 10 in that article. However, our results are slightly different, possibly due to differences in the input data or because some parts of the algorithm were not clearly described. Here we describe our procedure in relation to that described in Fossat *et al.* (2017).

We downloaded the 16.5-year-long time series of the solar global velocity observations from the GOLF instrument (García *et al.*, 2005) provided at www.ias.u-psud.fr/golf/templates/access.html and divided the data into eight-hour-long segments, which are offset by four hours. Thus, we have 36,130 segments at a four-hour cadence.

For each valid segment (with a duty-cycle greater than 25%) we first padded the data out to 10^6 seconds (about 35 times longer than the eight-hour-long segment) before computing the power spectrum. We filtered this power spectrum for the frequency band between 2.32 and 3.74 mHz, and we translated the beginning of this band to zero frequency. We subtracted the mean of the power spectrum and zero-padded out to 125 mHz (about 88 times the length of the frequency band). We then computed the power spectrum of this padded, frequency-filtered power spectrum to obtain the temporal power spectrum (which is the envelope of the autocorrelation of the GOLF time series in the selected frequency range). We performed a least-squares fit of a quadratic function to the prominent peak in the range between 14,000 seconds and 15,600 seconds. The time of the maximum of the quadratic is the round-trip travel-time of the p-modes. If the duty-cycle of a segment was less than 25%,

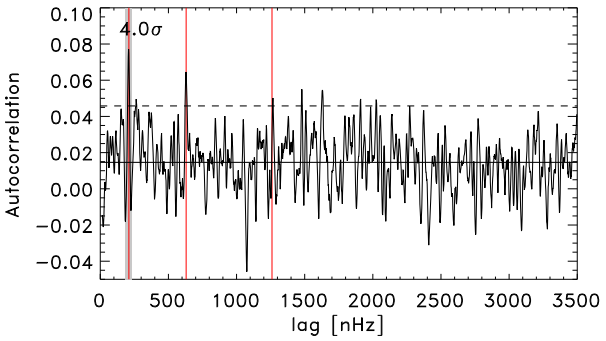

Figure 1 Autocorrelation of the power spectrum. This figure is directly comparable to Figure 10 in Fossat *et al.* (2017). The *red vertical lines* indicate the frequency splittings detected by Fossat *et al.* (2017) at 210, 630, and 1260 nHz. The *horizontal line* shows the mean of the autocorrelation, and the *dotted line* represents two standard deviations. We compute the significance of the maximum in the shaded region.

we set the measurement of the round-trip travel-time to zero. At this point, we have a time series of the round-trip travel-time of the p-modes at a four-hour cadence.

The condition that the segments have a minimum 25% duty-cycle was a subjective choice on our part because the value was not specifically stated in Fossat *et al.* (2017), and it results in 1.5% more round-trip travel-time measurements than Fossat *et al.* (2017). We have 34,723 non-zero values with a root-mean-square (rms) uncertainty of 54 seconds, compared to Figure 6 of Fossat *et al.* (2017), where the authors have 34,261 non-zero values with an rms of 52 seconds.

We then subtracted the mean value (14,806.3 seconds, compared to Fossat *et al.* (2017), who report 14,807 seconds) to obtain the round-trip travel-time perturbation as a function of time with a four-hour cadence. As in Fossat *et al.* (2017), we set the value of every data point with an absolute round-trip travel-time above 240 seconds (about a level of 5σ) to zero to remove outliers. We then computed the power spectrum of these round-trip travel-time perturbations and convolved it with a six-pixel-wide box-car window (11.5 nHz) to smooth the power spectrum, and calculated its autocorrelation up to 3500 nHz. We note that Fossat *et al.* (2017) used a seven-pixel-wide window with weighting [0.5, 1, 1, 1, 1, 1, 0.5] (E. Fossat, private communication, 2018). This makes little difference to the results.

Figure 1 shows the result of our analysis, which can be qualitatively compared to Figure 10 of Fossat *et al.* (2017). The peaks at 210 nHz, 630 nHz, and 1260 nHz are claimed by Fossat *et al.* (2017) to represent the splittings of the g-modes caused by rotation in the core. Our highest peak at 210 nHz has a significance of 4.0σ compared to 4.7σ in Fossat *et al.* (2017).

We defined the significance as the maximum value of the autocorrelation within 210 ± 25 nHz frequency lag (see the shaded region in Figures 1), relative to the standard deviation of the autocorrelation in the full range of frequency lag.

Here, we aimed to first reproduce the results qualitatively, and in the following sections, we analyse the sensitivity to some of the parameters in the analysis method.

Initially, we did not interpret the description of "smoothed over six bins" and "six-bin smoothing" of the power spectrum correctly and had difficulty acquiring the large significance of the main peak. Through private communication with D. Salabert and T. Corbard (2017), we established that this phrase means a convolution of a six-pixel-wide window with the power spectrum.

Fossat *et al.* (2017) showed in Figure 13 that the significance of the 210 nHz peak increases with the amount of GOLF data used. This is similar to changing either the 25% duty cycle condition and/or the 240 second cut-off, resulting in more or less valid round-trip travel-time measurements. We found that if we made this condition more stringent and used

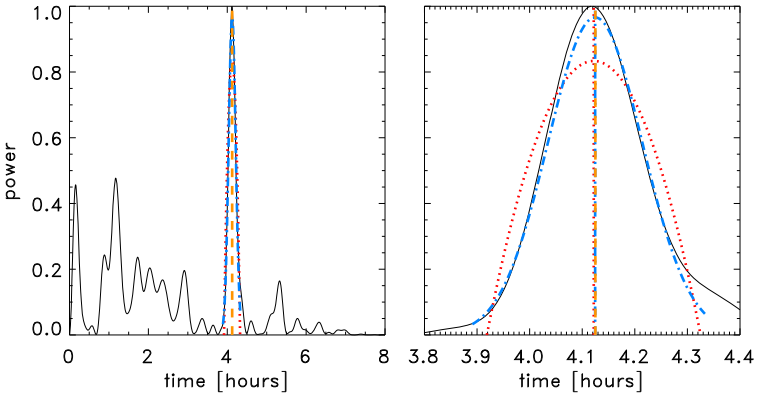

Figure 2 *Left*: Example temporal power spectrum of the fourth eight-hour-long segment showing the round-trip travel-time peak. This can be directly compared to Figure 4 in Fossat *et al.* (2017). The *red dotted curve* is the quadratic fit as described in Fossat *et al.* (2017), and the *blue dash–dotted curve* is a Gaussian fit. The *orange vertical dashed line* shows the location of the centroid. *Right*: Same as the left panel, but restricted to the time range used to measure the round-trip travel-time. The *vertical dashed lines* show the location of the measured round-trip travel-time for each measurement method. The location of the maxima of the quadratic (*red*, 14,838.7 seconds), the Gaussian (*blue*, 14,848.4 seconds), and centroid (*orange*, 14,849.9 seconds) are barely distinguishable on this scale.

a 50% duty cycle condition, there were 34,630 valid measurements of the round-trip travel-time and the significance of the 210 nHz peak was reduced to 3.7σ. Rather than trying to tune any of the criteria to increase the significance, we chose to keep a well-defined value in this article.

3. Sensitivity to the Method of Measuring the Round-Trip Travel-Time

Fossat *et al.* (2017) claimed that "the (second-order) polynomial fit made on a range of ± 800 seconds around 14,800 seconds minimizes the scatter of T", (where T is the round-trip travel-time), and that this fit is "not at all the best fit on the peak profile, but it is the least noisy estimate of the peak centroid."

Naively, it looks as though a Gaussian would be a good fit to measure the peak of this curve (see Figure 2), but the centroid may be the key parameter. Therefore we compared the least-squares fit of the quadratic function used by Fossat *et al.* (2017) [$q(t) = at^2 + bt + c$, where t is time] with a non-linear least-squares fit of a three-parameter Gaussian function [$g(t) = A\mathrm{e}^{(\frac{-(t-B)^2}{2C^2})}$] and with a direct measurement of the centroid [$\langle c \rangle = \frac{\int_{t_1}^{t_2} tT(t)\,\mathrm{d}t}{\int_{t_1}^{t_2} T(t)\,\mathrm{d}t}$, where $t_1 = 14{,}000$ seconds, $t_2 = 15{,}600$ seconds], and we evaluated the integrals discretely using the trapezoidal rule. Figure 2 shows an example of the different fits to the round-trip travel-time peak.

The rms of the round-trip travel-time perturbations (*e.g.* similar to Figure 1) is 53 seconds for the quadratic fit, 72 seconds for the Gaussian fit, and 64 seconds for the centroid measurement, compared to 52 seconds in Fossat *et al.* (2017). This quantitatively shows that the quadratic fit does indeed have the lowest noise compared to the two other methods of measuring the round-trip travel-time.

The Pearson correlation coefficient for the time series of the round-trip travel-time quadratic and Gaussian methods is 0.89, and the quadratic and centroid methods is 0.93,

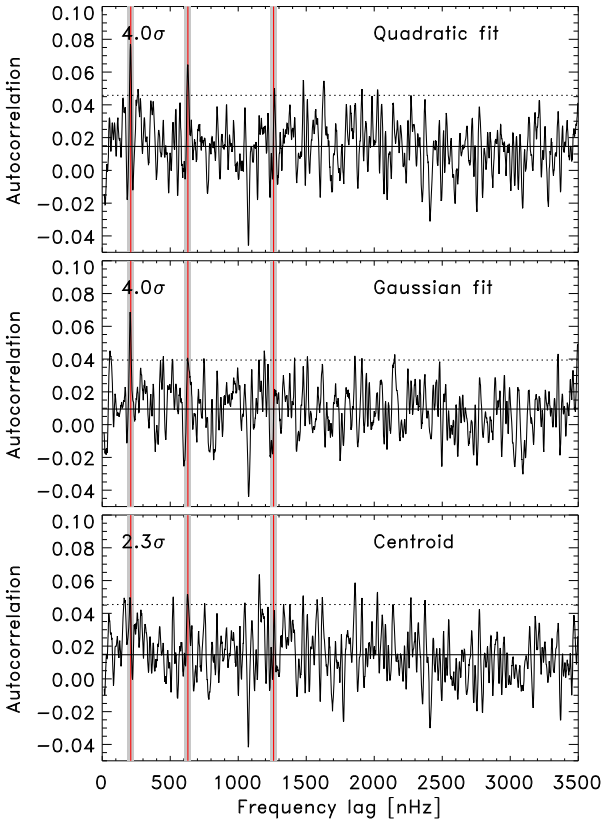

Figure 3 Autocorrelation function for the three different measurements of the round-trip travel-time (see Figure 2). The top panel shows the same as Figure 1, the middle panel presents the autocorrelation for the Gaussian fits, and the bottom panel shows the centroid measurement. The *red vertical lines* indicate the expected frequency splittings as reported by Fossat *et al.* (2017). The *horizontal line* shows the mean of the autocorrelation, and the *dotted line* represents two standard deviations. We compute the significance of the maximum in the grey shaded regions.

showing that measurements of the different methods do not differ greatly. The significance of the first peak in the autocorrelation function for the Gaussian is similar to the quadratic, but the second peak is not as significant, and the third peak is not clear at all (Figure 3). The first peak is much less significant in the centroid measurements than in the other two cases.

4. Sensitivity to the Smoothing of the Power Spectrum

Fossat *et al.* (2017) state that the significance of the peaks is maximised by convolving the power spectrum of the round-trip travel-times with a 6-pixel window (11.5 nHz, where one pixel corresponds to a frequency bin of 1.92 nHz) to smooth the data. They also state that the smoothing accounts for the imprecision of the observed mode frequencies in the power spectra. We computed the autocorrelation for power spectra convolved with box-car windows up to 12 pixels wide. Figure 4 shows the autocorrelation of the power spectrum without smoothing, and Figure 5 shows the autocorrelation of the power spectrum smoothed by a 12-pixel-wide (23 nHz) box-car window.

We computed the significance of the peaks in the autocorrelation by measuring the maximum value in the range 210 ± 25 nHz for the first peak, 630 ± 25 nHz for the second peak, and 1260 ± 25 nHz for the third peak (see, *e.g.* the shaded regions in Figure 3). Figure 6 shows the significance of each of the three peaks for different sizes of the smoothing

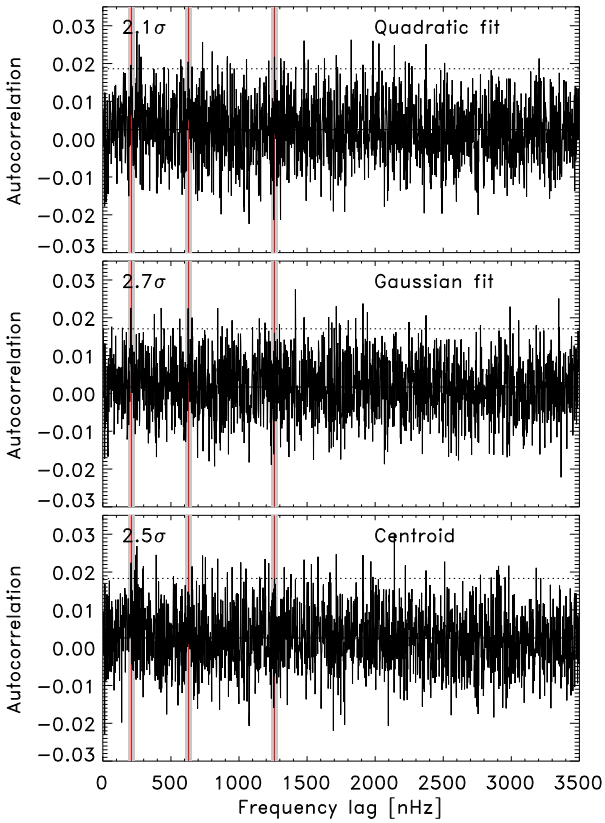

Figure 4 The autocorrelation of the power spectrum without any smoothing. The *vertical red lines* indicate the frequency splittings as reported by Fossat *et al.* (2017). The *horizontal line* is the mean of the autocorrelation and the *dotted line* represents two standard deviations. We compute the significance of the maximum in the grey shaded regions.

window and for the different methods of measuring the round-trip travel-time. We quantitatively show that the significance of the first and second peaks is maximum for a 6-pixel-wide smoothing window for the quadratic case that was reported by Fossat *et al.* (2017).

5. Sensitivity to the Start Time of the GOLF Time Series

The GOLF velocity time-series is 16.5 years long with an 80-second cadence. We changed the start time of the data by removing different amounts of data from the beginning of the time series to test the stability of the results.

Figure 7 shows the autocorrelation function for four different start times. When we removed two hours and ten hours, there were no significant peaks. On the other hand, removing whole segments (*e.g.* four or 24 hours) did not have a large effect on the significance of the peaks. The sensitivity to shifting the start time by several hours out of 16.5 years is a clear demonstration of the fragility of the results.

To further investigate the apparent dependence of the significance on multiples of four, we repeated the analysis after we removed shorter amounts of data. Figure 8 shows the significance of the three peaks as a function of the start time and reveals a four-hour oscillation period. The peak changes amplitude with a period of four hours because this is the equivalent of removing whole segments, *i.e.* an integer number of data points from the four-hour

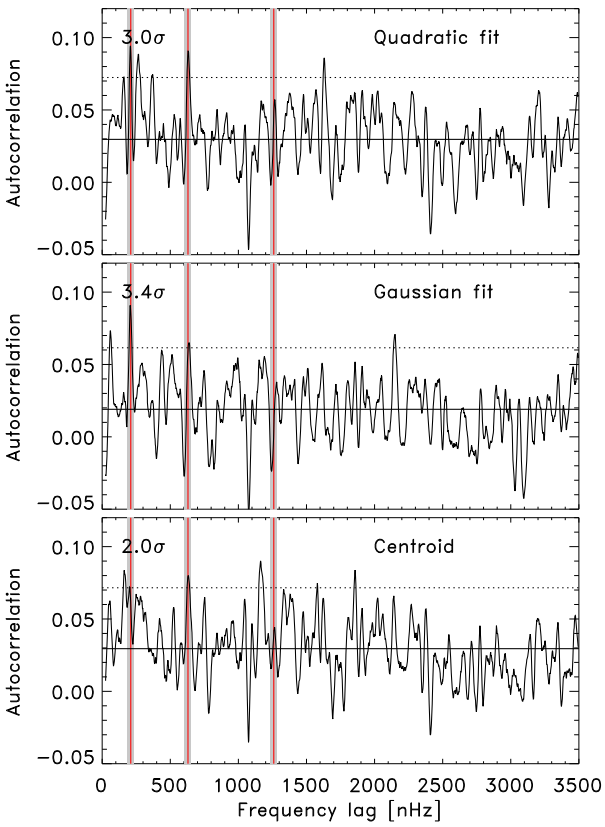

Figure 5 Autocorrelation of the power spectrum smoothed by 12 pixels (23 nHz). The *red vertical lines* indicate the frequency splittings reported by Fossat *et al.* (2017). The *horizontal line* shows the mean of the autocorrelation, and the *dotted line* represents two standard deviations. We compute the significance of the maximum in the grey shaded regions.

cadence round-trip travel-time measurement. The reported signal appears to be linked to a combination of the start time of the GOLF time series and the selected cadence of the round-trip travel-time measurement.

6. Sensitivity to the Cadence of the Round-Trip Travel-Time Measurement

Fossat *et al.* (2017) measured round-trip travel-times at a cadence of half (four hours) the segment length (eight hours). These appeared to be reasonable choices, but were not justified. In the previous section, we showed that the 210 nHz peak seems to be caused by some combination of the start time of the GOLF time series and the cadence of the round-trip travel-time measurements. We repeated the analysis using different values of the segment length. We kept the factor of two between the cadence and the segment length, such that the cadence of the round-trip travel-time measurement is half the segment length. We modified the cut-off value of 240 seconds by the relative rms of the non-zero round-trip travel-time for each cadence. Longer (shorter) segment lengths cause the round-trip travel-time peak to become more narrow (wider) and less (more) noisy.

In Figure 9 we show the autocorrelation function for several different cadences. The signal that is evident in the autocorrelation for a four-hour cadence vanishes for a 3.9 hour

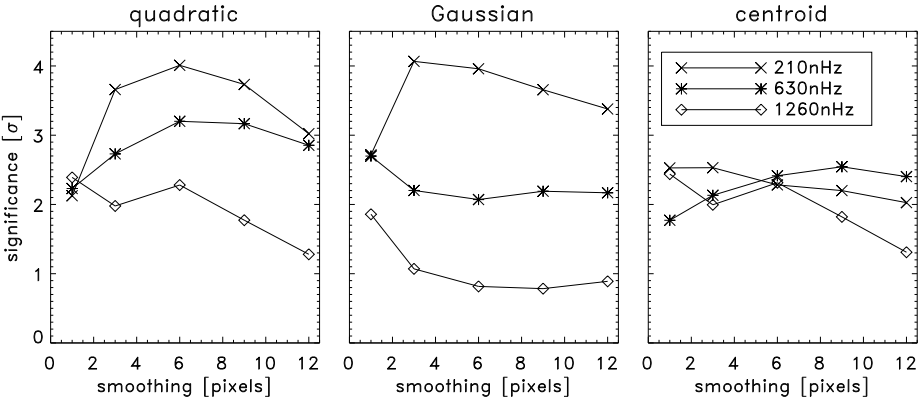

Figure 6 Significance of each of the peaks (shaded regions shown in Figures 3 and 4) as a function of the width of the smoothing window. The quadratic fit with a six pixel-wide smoothing window gives the highest significance for all peaks, in agreement with Fossat *et al.* (2017).

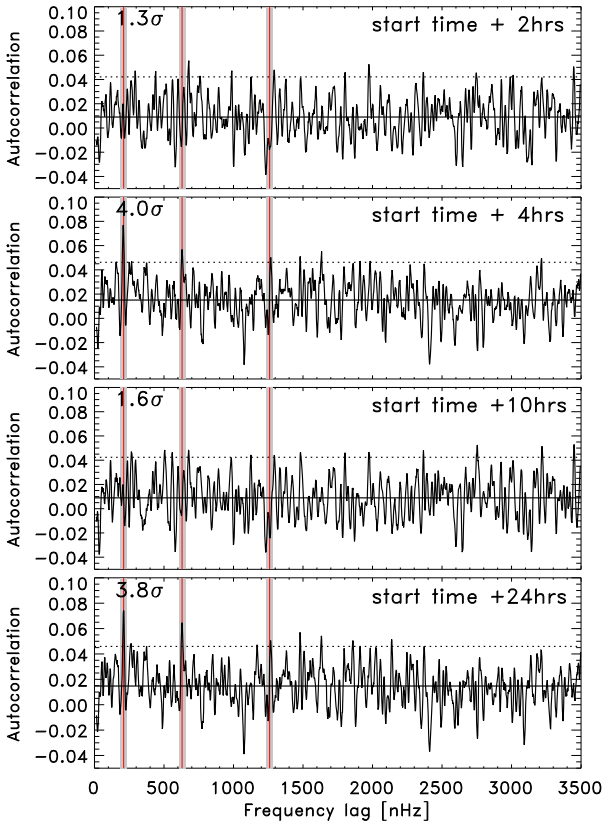

Figure 7 Autocorrelation function for start times offset by 2 hours (top), 4 hours, 10 hours, and 24 hours (bottom) relative to the original start time. We compute the significance of the maximum in the grey shaded regions. The *red vertical lines* indicate where Fossat *et al.* (2017) identified the original three g-mode peaks. Peaks at the location of the purported g-modes are only evident at multiples of 4 hours.

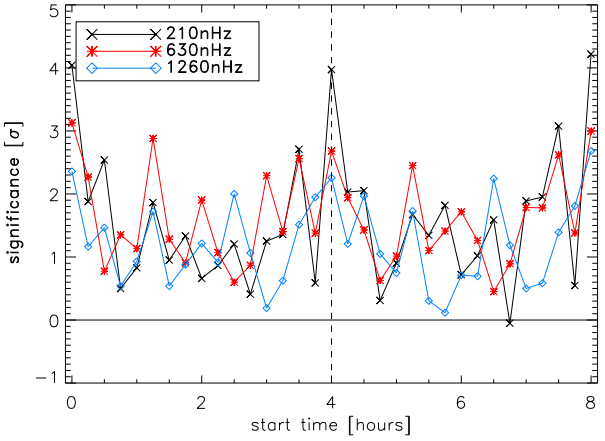

Figure 8 Significance of the three g-mode peaks as a function of start time relative to the original start time of the GOLF time series. The *black crosses* are the significance of the maximum value of the autocorrelation near the first peak, the *red stars* represent the significance near the second peak, and the *blue diamonds* show the significance near the third peak. The first points at zero start time correspond to the three peaks in Figure 1.

Figure 9 Autocorrelation function for different cadences of the round-trip travel-time measurement. From the top panel down, we show results for a 3 hour cadence, 3.5 hour cadence, 3.9 hour cadence, 4.5 hour cadence, and 5 hour cadence. We compute the significance of the maximum in the shaded regions. The *red vertical lines* indicate where Fossat *et al.* (2017) identified the original three g-mode peaks. The signal of the g-mode splittings has vanished in all cases.

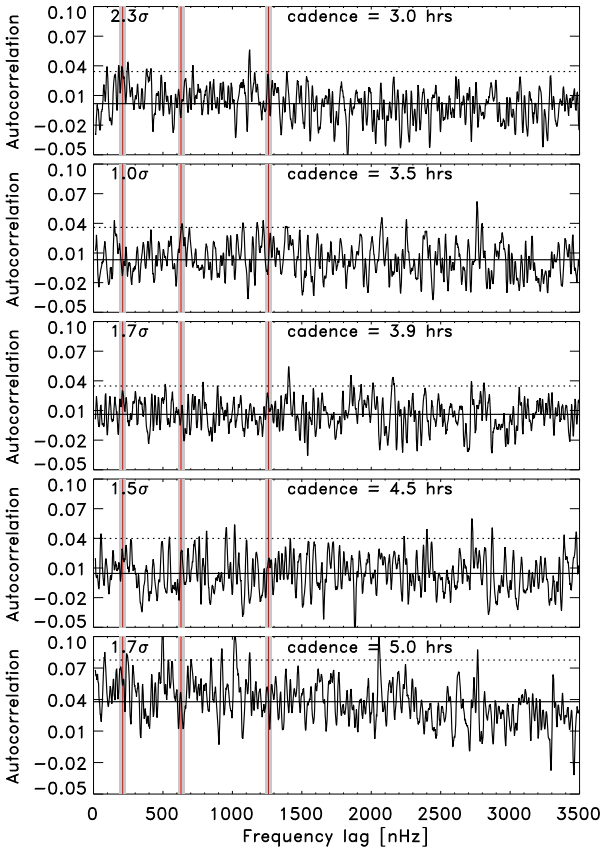

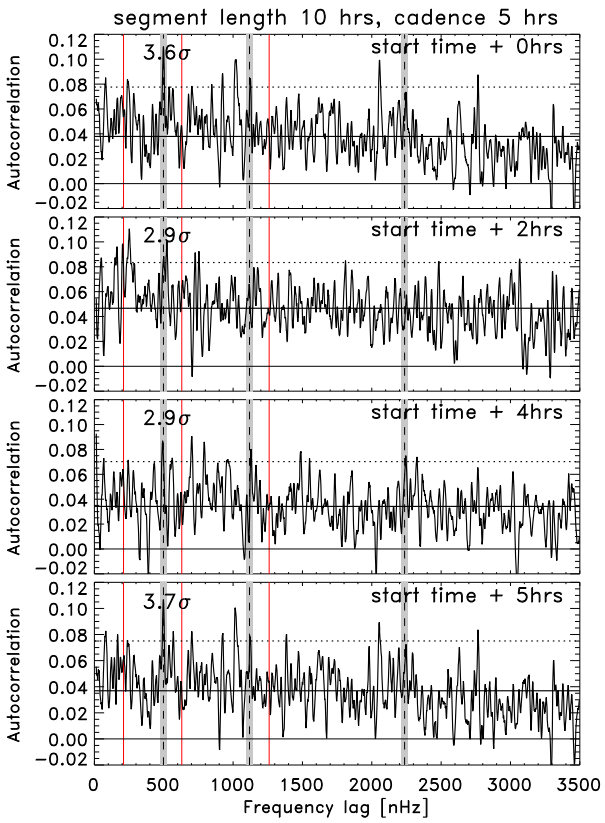

Figure 10 Autocorrelation function of round-trip travel-times made with a five-hour cadence for different start times offset by two, four, and five hours. The autocorrelation for no start time offset in the top panel is the same as in the bottom panel of Figure 9. The *red vertical lines* indicate where Fossat *et al.* (2017) identified the original three g-mode peaks. The *vertical dashed lines* show the location of the g-mode splittings we identified at the original start time (top panel) at 498 nHz, 1,118 nHz, and 2,237 nHz. We compute the significance of the maximum in the grey shaded regions.

cadence. Why such a small change has such a large impact is difficult to understand, as there is no particular physical relevance of four hours.

To further illustrate the robustness of the results, we explored what would happen if we were to initially select a different cadence. To do this, we chose the largest peak in the autocorrelation between 30 and 500 nHz and used this to compute where we would expect the other two peaks to be. To calculate where the other peaks should be, we used the asymptotic splitting of the g-modes: $s_{\ell,m} = m(\beta_\ell \Omega_g - \Omega_p)$, where $\beta_\ell = 1 - 1/(\ell(\ell+1))$, Ω_g is the mean rotation rate felt by the g-modes, and $\Omega_p = 433$ nHz is the mean rotation rate felt by the p-modes. For some cases we found peaks where we would expect them to be, although with a lower significance than for the four-hour cadence case. In other cases we did not find any significant peaks.

As an example, we show the case of measuring the round-trip travel-time at a five-hour cadence. We assumed that the largest peak that we found, at 498 nHz, is the $\ell = 1, m = 1$ mode, and so $\Omega_g = 1862$ nHz (4.3 times the rotation rate felt by the p-modes). Then we used this value of Ω_g to predict where the $\ell = 2$ mode splittings should be. These values, $s_{2,1} = 1118$ nHz and $s_{2,2} = 2237$ nHz, are shown as vertical dashed lines in the top panel of Figure 10, and indeed there are associated peaks. This demonstrates that if this arbitrary cadence had been chosen from the beginning, then a different answer would have been found.

We then adjusted the start time and repeated the analysis for the five-hour cadence (Figure 10). The bottom panel of Figure 10 shows the autocorrelation for a start time offset by

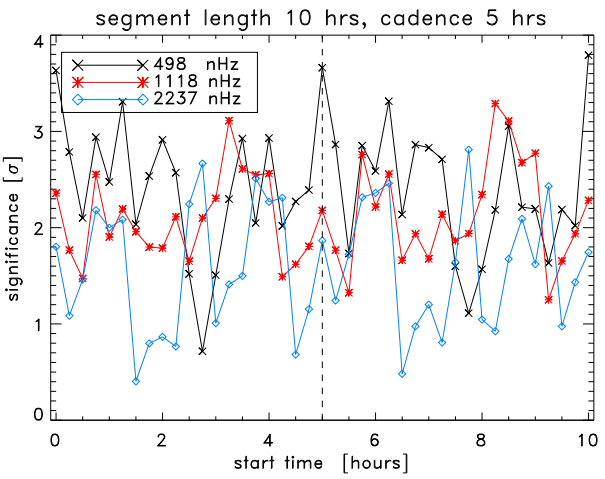

Figure 11 Same as Figure 8, except for segment lengths of ten hours and a cadence of five hours. The points at zero start time correspond to the three peaks in the top panel of Figure 10.

five hours (the cadence). We see that the locations of the peaks are similar to the case with no offset (top panel). Similar to the four-hour cadence case, Figure 11 shows that the significances are highest when integer multiples of the cadence are removed. Figures 8 and 11 together suggest that the peaks found by Fossat *et al.* (2017) could be an artefact of the analysis method and the choice of cadence.

7. Conclusions

We have shown that the most recent detection of g-modes by Fossat *et al.* (2017) is extremely fragile. In particular, the claimed detection is sensitive to

- the start time of the GOLF data series (Figure 7),
- the cadence of the round-trip travel-time measurements (Figure 9),
- the technique used to measure the round-trip travel-times (Figure 3), and
- the smoothing of the power spectrum (Figure 6).

The first point is worrying in particular because it means that a start time that is offset by a very small amount and excludes a very small fraction of the data makes a substantial difference, and it is worrying in general because the parameter is unrelated to the properties of the Sun. This is further illustrated in Figure 8, which shows that the significance varies with a period equal to the cadence of the data segments used. The latter two points, on the other hand, are less worrying, as they could in principle be attributed to properties of g-mode oscillations, even if the reason for the high sensitivity is not understood in detail. Overall, we conclude that the reported detection of g-modes must be treated with extreme caution until these issues are understood.

It would be valuable to repeat the analysis using other observational data sets from space (with the *Michelson Doppler Imager* onboard the *Solar and Heliospheric Observatory*, and with the *Helioseismic and Magnetic Imager* onboard the *Solar Dynamics Observatory)* and from the ground (with the *Birmingham Solar Oscillations Network* and the *Global Oscillation Network Group*).

We note that we have not investigated the further analyses by Fossat *et al.* (2017) and by Fossat and Schmider (2018), where they identify a model of the g-mode power spectrum in the observed power spectrum.

Acknowledgements Open access funding provided by Max Planck Society. We thank D. Salabert and T. Corbard for helping us to interpret the phrase "six-bin smoothing" in the article of Fossat *et al.* (2017), and E. Fossat for open and helpful discussions. This work was supported in part by the German Space Agency (Deutsches Zentrum für Luft- und Raumfahrt) under PLATO grant 50OO1501.

Disclosure of Potential Conflicts of Interest The authors declare that they have no conflicts of interest.

References

Appourchaux, T., Belkacem, K., Broomhall, A.-M., Chaplin, W.J., Gough, D.O., Houdek, G., Provost, J., Baudin, F., Boumier, P., Elsworth, Y., García, R.A., Andersen, B.N., Finsterle, W., Fröhlich, C., Gabriel, A., Grec, G., Jiménez, A., Kosovichev, A., Sekii, T., Toutain, T., Turck-Chièze, S.: 2010, The quest for the solar g modes. *Astron. Astrophys. Rev.* **18**, 197. DOI.

Fossat, E., Schmider, F.X.: 2018, More about solar g modes. *Astron. Astrophys.* **612**, L1. DOI.

Fossat, E., Boumier, P., Corbard, T., Provost, J., Salabert, D., Schmider, F.X., Gabriel, A.H., Grec, G., Renaud, C., Robillot, J.M., Roca-Cortés, T., Turck-Chièze, S., Ulrich, R.K., Lazrek, M.: 2017, Asymptotic g modes: Evidence for a rapid rotation of the solar core. *Astron. Astrophys.* **604**, A40. DOI.

Gabriel, A.H., Grec, G., Charra, J., Robillot, J.-M., Roca Cortés, T., Turck-Chièze, S., Bocchia, R., Boumier, P., Cantin, M., Cespédes, E., Cougrand, B., Crétolle, J., Damé, L., Decaudin, M., Delache, P., Denis, N., Duc, R., Dzitko, H., Fossat, E., Fourmond, J.-J., García, R.A., Gough, D., Grivel, C., Herreros, J.M., Lagardère, H., Moalic, J.-P., Pallé, P.L., Pétrou, N., Sanchez, M., Ulrich, R., van der Raay, H.B.: 1995, Global Oscillations at Low Frequency from the SOHO Mission (GOLF). *Solar Phys.* **162**, 61. DOI.

García, R.A., Turck-Chièze, S., Boumier, P., Robillot, J.M., Bertello, L., Charra, J., Dzitko, H., Gabriel, A.H., Jiménez-Reyes, S.J., Pallé, P.L., Renaud, C., Roca Cortés, T., Ulrich, R.K.: 2005, Global solar Doppler velocity determination with the GOLF/SoHO instrument. *Astron. Astrophys.* **442**, 385. DOI.

García, R.A., Turck-Chièze, S., Jiménez-Reyes, S.J., Ballot, J., Pallé, P.L., Eff-Darwich, A., Mathur, S., Provost, J.: 2007, Tracking solar gravity modes: The dynamics of the solar core. *Science* **316**, 1591. DOI.

Rauer, H., Catala, C., Aerts, C., Appourchaux, T., Benz, W., Brandeker, A., Christensen-Dalsgaard, J., Deleuil, M., Gizon, L., Goupil, M.-J., Güdel, M., Janot-Pacheco, E., Mas-Hesse, M., Pagano, I., Piotto, G., Pollacco, D., Santos, Ċ., Smith, A., Suárez, J.-C., Szabó, R., Udry, S., Adibekyan, V., Alibert, Y., Almenara, J.-M., Amaro-Seoane, P., Eiff, M.A.-v., Asplund, M., Antonello, E., Barnes, S., Baudin, F., Belkacem, K., Bergemann, M., Bihain, G., Birch, A.C., Bonfils, X., Boisse, I., Bonomo, A.S., Borsa, F., Brandão, I.M., Brocato, E., Brun, S., Burleigh, M., Burston, R., Cabrera, J., Cassisi, S., Chaplin, W., Charpinet, S., Chiappini, C., Church, R.P., Csizmadia, S., Cunha, M., Damasso, M., Davies, M.B., Deeg, H.J., Díaz, R.F., Dreizler, S., Dreyer, C., Eggenberger, P., Ehrenreich, D., Eigmüller, P., Erikson, A., Farmer, R., Feltzing, S., de Oliveira Fialho, F., Figueira, P., Forveille, T., Fridlund, M., García, R.A., Giommi, P., Giuffrida, G., Godolt, M., Gomes da Silva, J., Granzer, T., Grenfell, J.L., Grotsch-Noels, A., Günther, E., Haswell, C.A., Hatzes, A.P., Hébrard, G., Hekker, S., Helled, R., Heng, K., Jenkins, J.M., Johansen, A., Khodachenko, M.L., Kislyakova, K.G., Kley, W., Kolb, U., Krivova, N., Kupka, F., Lammer, H., Lanza, A.F., Lebreton, Y., Magrin, D., Marcos-Arenal, P., Marrese, P.M., Marques, J.P., Martins, J., Mathis, S., Mathur, S., Messina, S., Miglio, A., Montalban, J., Montalto, M., Monteiro, M.J.P.F.G., Moradi, H., Moravveji, E., Mordasini, C., Morel, T., Mortier, A., Nascimbeni, V., Nelson, R.P., Nielsen, M.B., Noack, L., Norton, A.J., Ofir, A., Oshagh, M., Ouazzani, R.-M., Pápics, P., Parro, V.C., Petit, P., Plez, B., Poretti, E., Quirrenbach, A., Ragazzoni, R., Raimondo, G., Rainer, M., Reese, D.R., Redmer, R., Reffert, S., Rojas-Ayala, B., Roxburgh, I.W., Salmon, S., Santerne, A., Schneider, J., Schou, J., Schuh, S., Schunker, H., Silva-Valio, A., Silvotti, R., Skillen, I., Snellen, I., Sohl, F., Sousa, S.G., Sozzetti, A., Stello, D., Strassmeier, K.G., Švanda, M., Szabó, G.M., Tkachenko, A., Valencia, D., Van Grootel, V., Vauclair, S.D., Ventura, P., Wagner, F.W., Walton, N.A., Weingrill, J., Werner, S.C., Wheatley, P.J., Zwintz, K.: 2014, The PLATO 2.0 mission. *Exp. Astron.* **38**, 249. DOI.